https://doi.org/10.46861/bmp.28.322 PŮVODNÍ PRÁCE/ORIGINAL PAPER

Crystal structure of uranyl-oxide mineral wölsendorfite revisited

Jakub Plášil

Fyzikální ústav AV ČR v.v.i., Na Slovance 2, 182 21 Praha 8; e-mail: plasil@fzu.cz

Plášil J (2020) Crystal structure of uranyl-oxide mineral wölsendorfite revisited. Bull Mineral Petrolog 28(2): 322-330 ISSN 2570-7337

Abstract

The crystal structure of the rare supergene Pb^{2+}-containing uranyl-oxide mineral wölsendorfite has been revisited employing the single-crystal X-ray diffraction. The new structure refinement provided deeper insight into the complex structure of this mineral, revealing additional H_2O sites in the interlayer complex and confirming the entrance of the Ca^{2+} into the structure. Studied wölsendorfite is orthorhombic, space group *Cmcm*, with unit cell dimensions *a* = 14.1233(8) Å, *b* = 13.8196(9) Å, *c* = 55.7953(12) Å, *V* = 10890.0(10) Å^3, and *Z* = 8. The structure has been refined to an agreement index (*R*) of 10.74% for 3815 reflections with $I > 3\sigma(I)$ collected using a microfocus X-ray source from the microcrystal. In line with the previous structure determination, the refined structure contains U–O–OH sheets of the wölsendorfite topology and an interstitial complex comprising nine symmetrically unique Pb sites, occupied dominantly by Pb^{2+}. Nevertheless, one of the sites seems to be plausible for hosting Ca^{2+}. Its presence has been successfully modeled by the refinement and further supported by the crystal-chemical considerations. The structural formula of wölsendorfite crystal studied is $Pb_{6.07}Ca_{0.68}[(UO_2)_{14}O_{18}(OH)_5]O_{0.5}(H_2O)_{12.6}$, with *Z* = 8, $D_{calc.}$ = 6.919 g·cm^{-3} (including theoretical 30.2 H atoms). The rather complex structure of wölsendorfite makes it the third most complex known uranyl-oxide hydroxy-hydrate mineral.

Keywords: *wölsendorfite, uranyl-oxide, crystal structure, Shinkolobwe, structure complexity, mineral associations*

Received 5. 10. 2020; accepted 12. 11. 2020

Introduction

Uranyl-oxide hydroxy-hydrates (further on abbreviated as UOHs) represent one of the most structurally and chemically complex families of naturally occurring U^{6+} phases (Plášil 2018), extremely important for the nuclear fuel waste management (see, e.g., O'Hare et al. 1988; Finch, Murakami 1999; Klingensmith et al. 2007; Kubatko et al. 2006; Maher et al. 2013; Ewing 2015). The onset of oxidation and hydration of uranium oxide, UO_2 (as pitchblende or synthetic in the nuclear fuel), often produces minerals consisting of electroneutral sheets of uranyl pentagonal bipyramids (of the α-U_3O_8 type) with substantial H_2O in the interlayer region, and typically little, if any, additional metal cations (Burns 2005; Krivovichev, Plášil 2013; Lussier et al. 2016; Plášil 2018a; Plášil et al. 2020). There are also particularly interesting rare cases when UOHs contain mixtures of U(IV), U(V), or U(VI) oxidation states as well (Burns et al. 1997; Burns, Finch 1999; Plášil 2017; Plášil et al. 2018). Continued alteration of uranium oxide, alteration in more chemically diverse aqueous fluids, and alteration of geologically old uranium oxide that contains substantial radiogenic lead result in the formation of uranyl-oxide hydroxy-hydrates with anionic sheets of uranyl polyhedra also containing uranyl square pyramids (β-U_3O_8 type of sheets) charge-balanced by cations in the interstitial regions of the structures.

Among UOHs there are several very complex minerals (following the terminology of Krivovichev 2013) that belong to the group of most complex minerals in Nature. Among them, there is also the uranyl-oxide mineral wölsendorfite, $(Pb_{6.16}Ba_{0.36})[(UO_2)_{14}O_{19}(OH)_4](H_2O)_{12}$, with 2885.80 bits/cell (Plášil 2018a) and a sizeable orthorhombic unit-cell with the *c* parameter having over 50 Å. Wölsendorfite has been described as a new mineral species from the Wölsendorf fluorite mining district in Bavaria, Germany, by Protas (1957). It has been reported from more than 30 localities worldwide then. Nevertheless, there is only one reliable full crystal structure determination and refinement (Burns 1999). Here, the second structure determination on the crystal of wölsendorfite from Shinkolobwe is given along with some summary of the mineral associations involved.

Sample

The crystal of wölsendorfite used in this study has been retrieved from the specimen on the holotype specimen of sayrite (RGM 13944), deposited in the collections of the Royal Museum for Central Africa in Tervuren (Belgium).

Single-crystal X-ray diffraction, structure refinement, and complexity calculations

A tabular fragment (0.058 mm × 0.041 mm × 0.006 mm) of a reddish wölsendorfite crystal was selected under a polarized-light microscope and mounted on a glass fiber. The X-ray data collection was done at room temperature with a Rigaku SuperNova single-crystal diffractometer (Mo*K*α radiation from a micro-focus X-ray tube collimated and monochromated by mirror-optics and detected by an Atlas S2 CCD detector). In line with the previous study by Burns (1999) wölsendorfite was found to be orthorhom-

Table 1 *Single-crystal data collection and structure-refinement details for wölsendorfite.*

Crystal data	
Structure formula	$Pb_{6.07}Ca_{0.68}[(UO_2)_{14}O_{18}(OH)_5]O_{0.5}(H_2O)_{12.60}$
Molecular weight	5672.22
Crystal system	orthorhombic
Space group	*Cmcm*
Unit-cell parameters: *a*, *b*, *c* [Å]	14.1233(8), 13.8196(9), 55.7953(12)
Unit-cell volume [Å^3]	10890.0(10)
Z	8
Calculated density [g/cm^3]	6.932 (for above mentioned formula)
Crystal size [mm]	0.058 × 0.041 × 0.006
F_{000}	18507
Data collection	
Diffractometer	Rigaku SuperNova with Atlas S2 detector
Temperature [K]	297
Radiation, wavelength [Å]	MoK_α, 0.71073 (50 kV, 30 mA)
θ range for data collection [°]	2.92 – 27.67
Limiting Miller indices	*h* = –18→17, *k* = –17→18, *l* = –72 → 73
Axis, frame width (º), time per frame (s)	ω, 1, 400
Total reflections collected	60978
Unique reflections	6673
Unique observed reflections, criterion	3815, [$I > 3\sigma(I)$]
Absorption coefficient [mm^{-1}], type	60.33; gaussian (Jana2006)
T_{min}/T_{max}	0.157/0.693
R_{int}	0.1524
Structure refinement by Jana2006	Full-matrix least-squares on F^2
Number of refined parameters, restraints, constraints	256, 0, 16
R, *wR* (obs)	0.1074, 0.1947
R, *wR* (all)	0.1817, 0.2260
GOF obs/all	1.87, 1.64
Weighting scheme, weights	σ, $w = 1/(\sigma^2(I)+0.0016I^2)$
Largest diffraction peak and hole (e$^-$/Å^3)	24.14 (0.48 Å close to O40), –18.46

Table 2 *Atom coordinates, displacement parameters (in Å^2) and occupation factors (occ.) for the structure of wölsendorfite.*

	x/a	*y/b*	*z/c*	U_{eq}/U_{iso}*	Occ.	U^{11}	U^{22}	U^{33}	U^{12}	U^{13}	U^{23}
U1	0.24034(10)	0.48484(9)	0.42479(3)	0.0080(2)		0.0132(5)	0.0057(4)	0.0051(4)	0.0022(3)	0.0001(3)	0.0028(3)
U2	0.24965(10)	0.27161(10)	0.46683(2)	0.0080(2)		0.0132(5)	0.0057(4)	0.0051(4)	0.0022(3)	0.0001(3)	0.0028(3)
U3	0.23896(10)	0.75363(10)	0.39339(2)	0.0080(2)		0.0132(5)	0.0057(4)	0.0051(4)	0.0022(3)	0.0001(3)	0.0028(3)
U4	0.23250(15)	1.28216(14)	0.25	0.0080(2)		0.0132(5)	0.0057(4)	0.0051(4)	0.0022(3)	0.0001(3)	0.0028(3)
U5	0.26001(11)	0.52782(10)	0.35864(2)	0.0070(4)		0.0129(9)	0.0055(7)	0.0025(7)	−0.0032(6)	−0.0037(5)	0.0024(5)
U6	0.25185(11)	0.74418(10)	0.31741(3)	0.0112(5)		0.0238(10)	0.0016(7)	0.0083(8)	−0.0016(6)	0.0029(7)	0.0013(6)
U7	0.23347(15)	0.5	0.5	0.0127(6)		0.0121(12)	0.0098(10)	0.0162(11)	0	0	−0.0068(9)
U8	0.23146(11)	1.00493(11)	0.28722(3)	0.0140(5)		0.0156(9)	0.0154(8)	0.0110(8)	0.0073(7)	−0.0013(6)	−0.0070(7)
Pb1	0	1.20064(18)	0.36224(5)	0.0245(9)	0.949(9)	0.0208(17)	0.0176(14)	0.0351(18)	0	0	0.0008(12)
Pb2	0	0.32995(18)	0.42343(5)	0.0273(10)	0.956(9)	0.0221(17)	0.0221(15)	0.038(2)	0	0	−0.0010(13)
Pb3	0	0.14630(19)	0.49981(5)	0.0279(10)	0.955(9)	0.0365(19)	0.0323(16)	0.0150(15)	0	0	−0.0025(13)
Pb4	0.5	1.08655(19)	0.31715(5)	0.0285(10)	0.936(9)	0.042(2)	0.0210(15)	0.0223(17)	0	0	−0.0021(12)
Pb5	0	0.82077(19)	0.42338(5)	0.0363(12)	0.926(9)	0.081(3)	0.0194(16)	0.0088(16)	0	0	0.0003(12)
Pb6	0.5	0.9624(3)	0.25	0.044(2)	0.865(13)	0.056(4)	0.031(3)	0.044(4)	0	0	0
Pb7/Ca7	0	1.1683(5)	0.28137(12)	0.052(3)	0.319(12) /0.681(12)	0.075(7)	0.063(6)	0.018(4)	0	0	−0.028(4)
Pb8	0	0.5988(13)	0.3924(4)	0.056(10)	0.156(10)	0.11(2)	0.023(11)	0.039(14)	0	0	0.017(9)
Pb9	0	0.9399(4)	0.25	0.068(3)	0.872(15)	0.108(6)	0.039(3)	0.056(5)	0	0	0

Table 2 *Atom coordinates, displacement parameters (in Å²) and occupation factors (occ.) for the structure of wölsendorfite - continuation.*

	x/a	*y/b*	*z/c*	U_{eq}/U_{iso}*	Occ.
O1	0.2423(18)	0.5967(17)	0.3956(5)	0.011(6)*	
O2	0.5	1.156(2)	0.2751(6)	0.009(8)*	
O3	0	0.647(2)	0.4418(6)	0.011(8)*	
O4	0.257(2)	0.849(2)	0.2876(6)	0.035(9)*	
O5	0.373(2)	0.7679(18)	0.3239(5)	0.022(7)*	
O6	0.137(2)	0.508(2)	0.3539(5)	0.031(8)*	
O7	0	1.126(2)	0.4074(6)	0.009(8)*	
O8	0.233(2)	0.433(2)	0.4631(5)	0.032(8)*	
O9	0.130(3)	0.244(3)	0.4650(7)	0.060(12)*	
O10	0.5	0.887(3)	0.2968(8)	0.036(12)*	
O11	0.207(2)	1.1602(19)	0.2773(5)	0.027(7)*	
O12	0.269(2)	0.580(2)	0.3219(5)	0.032(8)*	
O13	0.2095(19)	0.6321(17)	0.4446(4)	0.012(6)*	
O14	0	0.431(3)	0.4618(9)	0.043(13)*	
O15	0.271(3)	1.455(3)	0.25	0.039(13)*	
O16	0.1144(19)	0.4693(18)	0.4202(5)	0.018(7)*	
O17	0.366(2)	0.500(2)	0.4291(5)	0.025(7)*	
O18	0.267(2)	0.4101(19)	0.3871(5)	0.025(7)*	
O19	0.373(2)	0.296(2)	0.4683(5)	0.031(8)*	
O20	0.356(2)	1.025(2)	0.2849(5)	0.034(8)*	
O21	0.366(2)	0.757(2)	0.3900(5)	0.033(8)*	
O22	0.102(2)	0.985(2)	0.2871(6)	0.044(9)*	
O23	0.248(3)	0.817(3)	0.4279(7)	0.060(12)*	
O24	0	−0.009(3)	0.4648(8)	0.036(12)*	
O25	0.103(3)	1.309(3)	0.25	0.022(10)*	
O26	0.127(2)	0.7205(19)	0.3123(5)	0.022(7)*	
O27	0.5	0.171(3)	0.4920(8)	0.040(13)*	
O28	0	0.391(3)	0.3769(8)	0.036(12)*	
O29	0.231(2)	0.696(2)	0.3570(5)	0.034(9)*	
O30	0.387(2)	0.552(2)	0.3610(5)	0.030(8)*	
O31	0.235(2)	0.658(2)	0.4953(6)	0.044(10)*	
O32	0.2959(19)	0.3951(17)	0.3335(4)	0.013(6)*	
O33	0.5	1.209(3)	0.3523(8)	0.041(13)*	
O34	0	1.098(5)	0.3169(12)	0.02(2)*	0.60(10)
O35	0.354(3)	1.255(2)	0.25	0.014(9)*	
O36	0.110(2)	0.746(2)	0.3976(6)	0.036(9)*	
O37	0.105(4)	0.5	0.5	0.048(14)*	
O38	0.5	1.398(3)	0.3312(8)	0.034(12)*	
O39	0	0.845(3)	0.2155(8)	0.038(13)*	
O40	0	1.094(4)	0.25	0.038(18)*	
O41	0.357(4)	0.5	0.5	0.058(16)*	
O42	0	0.912(3)	0.3868(9)	0.049(15)*	

bic, a = 14.1233(8) Å, b = 13.8196(9) Å, c = 55.7953(12) Å, V = 10890.0(10) Å³, and Z = 8. Integration of the diffraction data, including corrections for background, polarization and Lorentz effects, were carried out with the CrysAlis RED program (Rigaku 2019). A gaussian absorption correction using refined crystal shape (using X-SHAPE program) was applied to data in the Jana2006 software, optimized by spherical harmonics (Petříček et al. 2014). Crystallographic data and experimental details are given in Table 1. The structure of wölsendorfite was solved independently from the previous determination utilizing the charge-flipping algorithm of the SHELXT program (Sheldrick 2015). Therefore, also the atom numbering scheme is distinct from that given by Burns (1999). Structure refinement was done using the software Jana2006 with the full-matrix least-squares refinement based on F^2. The structure refinement confirmed the choice of the *C*-centered orthorhombic cell and the space group *Cmcm*. The structure solution revealed positions for all U-atoms within the structure sheet and nearly all of the Pb atoms in the interlayer (except for those only low-populated); the sheet's completion required the localization of O atoms from the difference Fourier maps. Nevertheless, despite the data quality, localization was straightforward. The final structure refinement returned higher but still satisfactory *R*-values, R = 10.84% and wR = 19.64% for 3185 unique observed reflections, fulfilling the criterion for observed intensities $I_{obs} > 3\sigma(I)$. We have to keep in mind the number of heavy atoms in, nevertheless, the large unit cell, leading to the immense absorption for X-rays (μ = 60.77 mm^{-1}) and consequent problems with the low intensities and proportionally large experimental errors. The weak intensities and poorer absorption correction are also the reason for both weakly negative (U1 and U2) and significantly small but positive (for instance, U3, O1, O2) values of equivalent atomic displacement parameters; the final fit thus treated them equally. It was not possible to discern reliably the amount of possibly entering Ba to the certain atomic site. Nevertheless, based on further crystal-chemical considerations (see below), the conclusion made is that currently studied wölsendorfite is possibly Ba-free. Final atom coordinates are given in Table 2, selected interatomic distances in Table 3, and the results of the bond-valence analysis in Table 4. Crystallographic data (CIF) are available as supplementary material online.

In order to evaluate the structural complexity of wölsendorfite, the information-based approach developed by Krivovichev (2012, 2013, 2014, 2016) and recently used for determination of structural complexity of U^{6+} oxysalts elsewhere (e.g., Gurzhiy, Plášil 2019; Gurzhiy et al. 2019; Kornyakov et al. 2020; Plášil 2018a) has been used. The structural complexity is quantitatively estimated as a Shannon information content (in bits) per atom (I_G) and per unit cell ($I_{G,total}$).

Refined crystal structure of wölsendorfite

The large unit cell of wölsendorfite (Fig. 1) contains eight distinct U sites, further on, it contains eight Pb and thirty-two O sites (plus H-sites, which, nevertheless, have not been revealed by the current refinement).

In wölsendorfite, all U sites are occupied by U^{6+}, according to the bond-valence analysis (Tab. 4). The U^{6+} cation is strongly bonded by the triple bonds to two O atoms, forming nearly linear $(UO_2)^{2+}$ uranyl ions. The U–O_{Ur} bond-lengths are ~1.8 Å, except of U2 and U4 sites (Tab. 3); however, it is most probably due to poorer absorption correction. Despite that, all refined bond-lengths

lie within the range of bond-lengths obtained from the well-refined structures (Lussier et al. 2016). The uranyl ions are further coordinated by four or five equatorial ligands, resulting in $Ur\Phi_4$ square bipyramids and $Ur\Phi_5$ pentagonal bipyramids, respectively (where Φ denotes an unspecified ligand). Uranyl ion at the U3 and U7 sites is coordinated by four O atoms; the remaining uranyl ions are each coordinated by five anions (Tab. 3 and 4).

As mentioned by Burns (1999), one of the U^{6+}-coordination polyhedrons contains U^{6+}–$(OH)_{eq}$ separation peculiarly long. In the case of wölsendorfite studied by Burns (1999) it was 3.06 Å. The conclusion made that it goes about the weak bond, considerably longer than most U^{6+}–Φ_{eq} bonds. Moreover, a similar finding was made by Pagoaga et al. (1987) (3.02 Å) and also by Finch et al. (2006) (3.097 Å) for the structure of billietite. The peculiarly long U–OH bond is confirmed by the current study: the U8 polyhedra contains U8–O32 bond, 3.026 Å long (Tab. 3, contributing 0.13 *vu* to the central U8 atom (Tab. 5).

Table 3 *Interatomic distances among U^{6+} polyhedra (in Å) in the structure of wölsendorfite.*

U1–O1	2.25(3)	U2–O8	2.25(3)
U1–O8	2.26(3)	U2–O9	1.74(4)
U1–O13	2.35(3)	U2–O13^{i}	2.36(3)
U1–O16	1.82(3)	U2–O19	1.78(3)
U1–O17	1.80(3)	U2–O23^{i}	2.26(4)
U1–O18	2.37(3)	U2–O31^{ii}	2.34(3)
U1–O23^{i}	2.33(4)	U2–O31^{i}	2.24(3)
<U1–O_{Ur}>	1.82	<U2–O_{Ur}>	1.76
<U1–O_{eq}>	2.31	<U2–O_{eq}>	2.29
U3–O1	2.17(3)	U4–O4^{iv}	2.30(3)
U3–O18^{iii}	2.19(3)	U4–O4^{iii}	2.30(3)
U3–O21	1.80(3)	U4–O11	2.30(3)
U3–O23	2.12(4)	U4–O11^{v}	2.30(3)
U3–O29	2.18(3)	U4–O15	2.45(4)
U3–O36	1.84(3)	U4–O25	1.87(4)
<U3–O_{Ur}>	1.82	U4–O35	1.76(4)
<U3–O_{eq}>	2.17	<U4–O_{Ur}>	1.81
		<U4–O_{eq}>	2.33
U5–O1	2.29(2)	U6–O4	2.21(3)
U5–O6	1.78(3)	U6–O5	1.78(3)
U5–O12	2.18(3)	U6–O11^{i}	2.59(3)
U5–O18	2.28(3)	U6–O12	2.30(3)
U5–O29	2.36(3)	U6–O26	1.82(3)
U5–O30	1.83(3)	U6–O29	2.33(3)
U5–O32	2.37(3)	U6–O32^{iii}	2.37(3)
<U5–O_{Ur}>	1.82	<U6–O_{Ur}>	1.81
<U5–O_{eq}>	2.30	<U6–O_{eq}>	2.36
U7–O8	2.26(3)	U8–O4	2.18(3)
U7–O8^{ii}	2.26(3)	U8–O11	2.24(3)
U7–O31	2.20(3)	U8–O12^{iii}	2.20(3)
U7–O31^{ii}	2.20(3)	U8–O15^{vi}	2.188(13)
U7–O37	1.81(6)	U8–O20	1.78(3)
U7–O41	1.74(6)	U8–O22	1.85(3)
<U7–O_{Ur}>	1.78	U8–O32^{iii}	3.02(3)
<U7–O_{eq}>	2.23	<U8–O_{Ur}>	1.82
		<U8–O_{eq}>	2.37

Symmetry codes: (i) –*x*+1/2, *y*–1/2, *z*; (ii) *x*, –*y*+1, –*z*+1; (iii) –*x*+1/2, *y*+1/2, *z*; (iv) –*x*+1/2, *y*+1/2, –*z*+1/2; (v) *x*, *y*, –*z*+1/2; (vi) –*x*+1/2, *y*–1/2, –*z*+1/2.

Table 4 *Interatomic distances among Pb^{2+} polyhedra (in Å) in the structure of wölsendorfite.*

Pb1–O5^{vii}	2.94(3)	Pb2–O7^{ix}	2.96(3)
Pb1–O5^{iii}	2.94(3)	Pb2–O9	3.19(4)
Pb1–O7	2.72(3)	Pb2–O9^{x}	3.19(4)
Pb1–O21^{vii}	2.57(3)	Pb2–O14	2.56(4)
Pb1–O21^{iii}	2.57(3)	Pb2–O16	2.51(3)
Pb1–O28^{viii}	2.76(4)	Pb2–O16^{x}	2.51(3)
Pb1–O30^{vii}	2.60(3)	Pb2–O21^{xi}	2.84(3)
Pb1–O30^{iii}	2.60(3)	Pb2–O21^{i}	2.84(3)
Pb1–O34	2.90(6)	Pb2–O28	2.73(4)
<Pb1–O>	2.73	<Pb2–O>	2.81
Pb3–O9	2.99(4)	Pb4–O2	2.53(3)
Pb3–O9^{x}	2.99(4)	Pb4–O6^{xv}	3.02(3)
Pb3–O19^{xii}	2.65(3)	Pb4–O6^{iii}	3.02(3)
Pb3–O19^{xiii}	2.65(3)	Pb4–O10	2.98(4)
Pb3–O24	2.90(4)	Pb4–O20	2.85(3)
Pb3–O24^{xiv}	2.74(4)	Pb4–O20^{xvi}	2.85(3)
Pb3–O27^{xii}	2.57(4)	Pb4–O26^{xv}	2.60(3)
Pb3–O41^{xi}	2.86(4)	Pb4–O26^{iii}	2.60(3)
Pb3–O41^{xiii}	2.86(4)	Pb4–O33	2.59(4)
<Pb3–O>	2.80	<Pb4–O>	2.78
Pb5–O3	2.61(3)	Pb6–O2	3.02(3)
Pb5–O17^{vii}	3.13(3)	Pb6–O2^{xvii}	3.02(3)
Pb5–O17^{iii}	3.13(3)	Pb6–O10	2.81(4)
Pb5–O19^{vii}	3.10(3)	Pb6–O10^{xvii}	2.81(4)
Pb5–O19^{iii}	3.10(3)	Pb6–O20	2.95(3)
Pb5–O24^{viii}	3.30(4)	Pb6–O20^{xvii}	2.95(3)
Pb5–O36	2.36(3)	Pb6–O20^{v}	2.95(3)
Pb5–O36^{x}	2.36(3)	Pb6–O20^{xvi}	2.95(3)
Pb5–O42	2.40(5)	Pb6–O25^{xviii}	2.57(4)
<Pb5–O>	2.83	Pb6–O25^{vi}	2.57(4)
		<Pb6–O>	2.84
Pb7/Ca7–O5^{xii}	3.28(3)	Pb8–O1	3.42(3)
Pb7/Ca7–O5^{iii}	3.28(3)	Pb8–O1^{x}	3.42(3)
Pb7/Ca7–O10^{xi}	3.14(4)	Pb8–O3	2.83(4)
Pb7/Ca7–O11	2.93(3)	Pb8–O6	3.15(3)
Pb7/ Ca7–O11^{x}	2.93(3)	Pb8–O6^{x}	3.15(3)
Pb7 /Ca7–O22	2.93(3)	Pb8–O16	2.87(3)
Pb7/ Ca7–O22^{x}	2.93(3)	Pb8–O16^{x}	2.87(3)
Pb7/ Ca7–O25	2.99(3)	Pb8–O28	3.00(4)
Pb7/ Ca7–O25^{xix}	2.99(3)	Pb8–O33^{xi}	2.70(5)
Pb7/ Ca7–O34	2.21(6)	Pb8–O36	2.57(3)
Pb7/ Ca7–O40	2.03(3)	Pb8–O36^{x}	2.57(3)
<Pb7/ Ca7–O>	2.88	<Pb8–O>	2.95
Pb9–O35^{xi}	3.28(3)		
Pb9–O35^{vi}	3.28(3)		
Pb9–O39	2.33(4)		
Pb9–O39^{xix}	2.33(4)		
Pb9–O40	2.13(6)		
Pb9–O22	2.60(3)		
Pb9–O15^{xv}	3.24(4)		
<Pb9–O>	2.74		

Symmetry codes: (i) –*x*+1/2, *y*–1/2, *z*; (iii) –*x*+1/2, *y*+1/2, *z*; v) *x*, *y*, –*z*+1/2; (vi) –*x*+1/2, *y*–1/2, –*z*+1/2; (vii) *x*–1/2, *y*+1/2, *z*; (viii) *x*, *y*+1, *z*; (ix) *x*, *y*–1, *z*; (x) –*x*, *y*, *z*; (xi) *x*–1/2, *y*–1/2, *z*; (xii) *x*–1/2, –*y*+1/2, –*z*+1; (xiii) –*x*+1/2, –*y*+1/2, –*z*+1; (xiv) *x*, –*y*, –*z*+1; (xv) *x*+1/2, *y*+1/2, *z*; (xvi) –*x*+1, *y*, *z*; (xvii) –*x*+1, *y*, –*z*+1/2; (xviii) *x*+1/2, *y*–1/2, *z*; (xix) –*x*, *y*, –*z*+1/2.

There are eight symmetrically distinct Pb-sites in the interlayer (Fig. 2). The polyhedral geometries (Tab. 4) and bond-valence sums incident upon those sites (Tab. 5) are consistent with all Pb present as Pb^{2+}, as is the case for all known Pb-containing uranyl-oxide hydroxy -hydrate minerals (Plášil 2018). According to site-scattering refinement results, some of the sites (Pb7 and Pb8) are considerably low-populated, <0.5. Unlike the conclusion made by Burns (1999), one of the sites in the crystal studied by him, the Pb8 site is a mix-site containing both Pb and Ba, wölsendorfite studied by the current study probably does not contain Ba at all, or only marginally. The argument of Burns (1999) was, besides the refinement, geometrical: conforming the larger average Pb8–Φ bond-length with the larger ionic radius of Ba^{2+} over Pb^{2+} (Shannon 1976). For instance, $^{[10]}Pb^{2+}$ has ionic radius of 1.4 Å, while $^{[10]}Ba^{2+}$ has 1.5 Å. The comparison of corresponding Voronoi-Dirichlet polyhedral (VDP) volumes for the Pb^{2+}-coordination polyhedra in wölsendorfite studied by Burns (1999) clearly shows that Pb8/Ba8 polyhedron is considerably larger (22.77 $Å^3$) than the average volume, V_{VDP} = 17.06 $Å^3$, of the remaining polyhedra. Any similar larger polyhedra are not present in the currently studied structure (Tab. 6). Therefore the conclusion is that the currently studied wölsendorfite is Ba-free. Moreover, based on the smaller volume of the Pb7 and the fact that the studied crystal comes in the Ca-rich association, this site has been treated as a mixed Pb/Ca site (Tab. 2 and 5). As all Pb polyhedra in the interlayer of wölsendorfite (Fig. 2) are fairly irregular, and some are distinctly one-sided, it suggests that the Pb^{2+} cations are lone-pair stereoactive.

In contrast to the structure given by Burns (1999) there are some substantial differences obtained from the current refinement. It has revealed two additional O sites that belong to H_2O and different proportions of the O and OH within the sheet. The sum of the H_2O, based on the refined occupancies of those sites that were partially occupied (based on the high U_{iso} values at first), is 12.85 H_2O per unit cell, for Z = 8. Based on the bond-valence analysis, it is likely that there could be 5 OH and 18 O within the layer, giving a net charge of –13, in contrast to the net charge –14 by Burns (1999). One of the O atoms, O40, which is a ligand of Pb7/Ca7 and Pb9 polyhedra, seems to be O^{2-} (sum of BV ~1.6 *vu*), most probably accepting one additional weak H-bond to meet its BV requirements. Considering this, there is an additional 0.5O in the interlayer (O40 had a multiplicity of 4). The formula for the wölsendorfite crystal studied can be written as $Pb_{6.07}Ca_{0.68}[(UO_2)_{14}O_{18}(OH)_5]O_{0.5}(H_2O)_{12.6}$, with Z = 8, $D_{calc.}$ = 6.919 g cm^{-3} (including theoretical 30.2 H atoms). This formula has a net charge of –0.50, indicating that there can be some O↔OH substitution within the structure sheets. Another possibility is that O40 is the OH group instead (the shorter Pb7–O40 would be an artifact of the poorer fit). The corresponding formula is then $Pb_{6.07}Ca_{0.68}[(UO_2)_{14}O_{18}(OH)_5]OH_{0.5}(H_2O)_{12.6}$, which is electroneutral.

Complexity of wölsendorfite in comparison with other UOHs

In general, some of UOHs are among the very complex minerals, considering the categories established by Krivovichev (2013). So far, the most complex UOH mineral (Tab. 7) is vandendriesscheite, $Pb_{1.5}[(UO_2)_{10}O_6(OH)_{11}]$

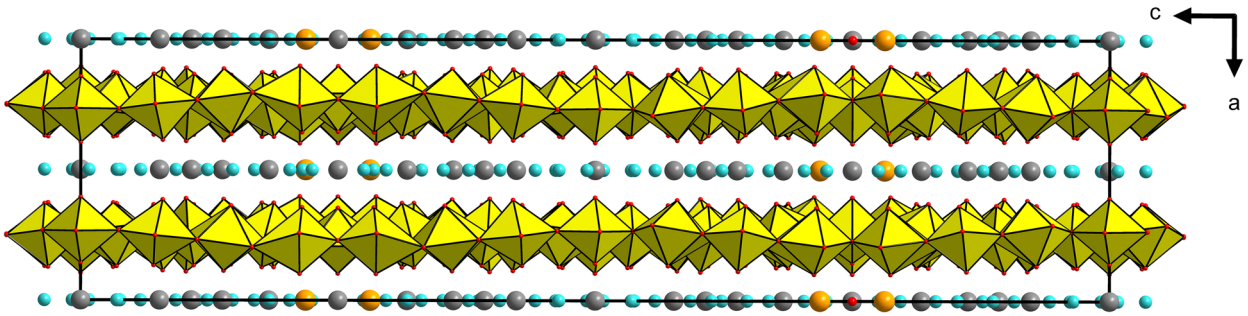

Fig. 1 *Crystal structure of wölsendorfite, view down [010]. Uranyl polyhedra are yellow, O atoms are represented by red circles, H_2O groups as azure circles, Pb^{2+} grey and Ca^{2+}-populated sites orange. Unit-cell edges are outlined as black-solid lines.*

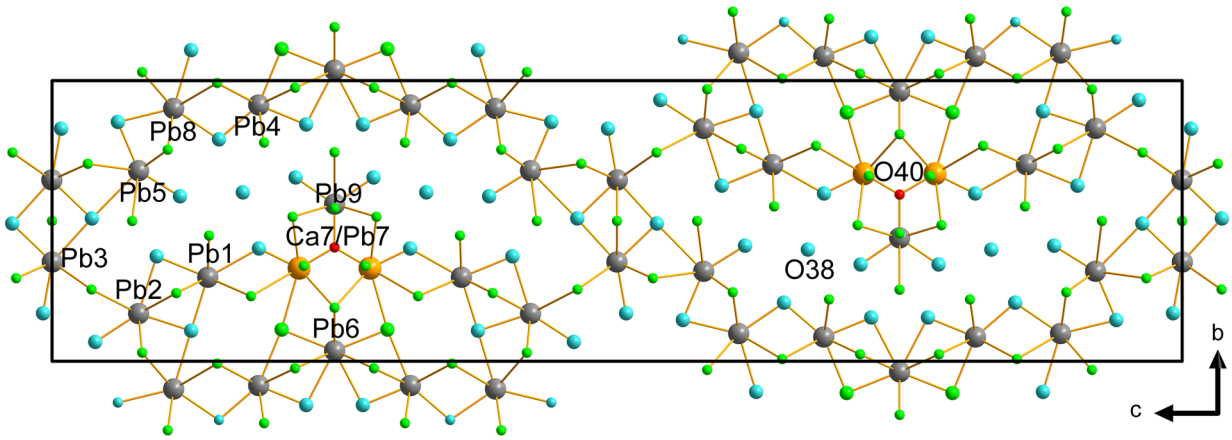

Fig. 2 *Interlayer complex in the studied wölsendorfite, view down [100]. Pb^{2+} sites are in grey and Ca^{2+}-populated sites in orange color; O sites that are ligands of the U-polyhedra are displayed as green spheres; H_2O groups are azure. Unit-cell edges are outlined as black-solid lines.*

$(H_2O)_{11}$ (Burns 1997). This mineral appears relatively soon in the alteration sequence after uraninite (Finch, Ewing 1992; Plášil 2018) and is characteristic for the presence of Pb^{2+}, usually of the radiogenic origin, derived from weathered pitchblende. The second most complex mineral is gauthierite, $KPb[(UO_2)_7O_5(OH)_7](H_2O)_8$ (Olds et al. 2017a), which seems to appear relatively soon in the sequence after vandendriesscheite. Its structure is based on its own topology, called gauthierite topology, which resembles vandendriesscheite, but it has a shorter sequence. The structure contains additional cation, K^+, but on the other hand, has a lower molar proportion of H_2O. The third most complex UOH has to be newly considered wölsendorfite. This study revealed additional H_2O sites, and both richetite and schoepite that had been considered in the past as far more complex turned out to be less-complex actually as they have been structurally revisited (Plášil 2017, 2018). For comparison, the most complex mineral in Nature is the uranyl carbonate ewingite (Olds et al. 2017b), $Mg_8Ca_8(UO_2)_{24}(CO_3)_{30}O_4(OH)_{12}(H_2O)_{138}$. This mineral is not, however, based on sheets of uranyl polyhedra, like UOHs, but it contains nano-sized metal-oxo clusters that, so far, have no close chemical or topological analogs in synthetic chemistry. The information content of 23477.51 bits/cell (including H atoms) makes it the most complex mineral (Krivovichev 2020).

Table 5 *Bond-valence analysis for the structure of wölsendorfite.*

	U1	U2	U3	U4	U5	U6	U7	U8	Pb1	Pb2	Pb3	Pb4	Pb5	Pb6	Pb7/ Ca7	Pb8	Pb9	ΣBV	Assign-ment
O1	0.65		0.77		0.60											0.05$^{\times 2\downarrow}$		2.06	O
O2												0.32		0.11$^{\times 2\downarrow}$				0.27	H_2O
O3													0.27			0.16		0.43	H_2O
O4				0.59$^{\times 2\downarrow}$		0.71		0.75										2.04	O
O5						1.75			0.13$^{\times 2\downarrow}$						0.05$^{\times 2\downarrow}$			1.93	O
O6					1.75							0.11$^{\times 2\downarrow}$				0.08$^{\times 2\downarrow}$		1.94	O
O7									0.21	0.12								0.33	H_2O
O8	0.64	0.65					0.64$^{\times 2\downarrow}$											1.92	O
O9		1.91								0.07$^{\times 2\downarrow}$	0.12$^{\times 2\downarrow}$							2.10	O
O10												0.12		0.17$^{\times 2\downarrow}$	0.06			0.34	H2O
O11				0.59$^{\times 2\downarrow}$		0.32		0.66							0.10$^{\times 2\downarrow}$			1.66	O
O12					0.75	0.58		0.72										2.06	O
O13	0.53	0.51																1.04	OH
O14										0.30								0.30	H_2O
O15				0.43				0.74									0.07	1.23	OH
O16	1.61									0.34$^{\times 2\downarrow}$						0.15$^{\times 2\downarrow}$		2.10	O
O17	1.68												0.08$^{\times 2\downarrow}$					1.77	O
O18	0.50		0.74		0.61													1.85	O
O19		1.75									0.25$^{\times 2\downarrow}$		0.09$^{\times 2\downarrow}$					2.09	O
O20								1.75				0.16$^{\times 2\downarrow}$		0.13$^{\times 4\downarrow}$				2.16	O
O21			1.68						0.30$^{\times 2\downarrow}$	0.16$^{\times 2\downarrow}$								2.14	O
O22								1.51							0.10$^{\times 2\downarrow}$		0.28	1.89	O
O23	0.55	0.64	0.86															2.04	O
O24											0.14; 0.20		0.06					0.23	H_2O
O25				1.45										0.30$^{\times 2\downarrow}$	0.09$^{\times 2\downarrow}$			1.83	O
O26						1.61						0.28$^{\times 2\downarrow}$						1.89	O
O27											0.30							0.30	H_2O
O28									0.19	0.21						0.11		0.51	H_2O
O29			0.75		0.51	0.55												1.82	O
O30					1.58				0.28$^{\times 2\downarrow}$									1.86	O
O31		0.54; 0.66					0.72$^{\times 2\downarrow}$											1.32	O
O32					0.50	0.50		0.13										1.14	OH
O33												0.28				0.22		0.50	H_2O
O34									0.14						0.54			0.68	H_2O
O35				1.83													0.06$^{\times 2\downarrow}$	1.89	O
O36			1.55										0.48$^{\times 2\downarrow}$			0.30$^{\times 2\downarrow}$		2.32	O
O37							1.65											1.65	O
O38																		0.00	H_2O
O39																	0.51$^{\times 2\downarrow}$	0.51	H_2O
O40															0.82		0.80	1.63	O
O41							1.91				0.15$^{\times 2\downarrow}$							2.06	O
O42													0.43					0.43	H_2O
	6.16	6.67	6.34	6.05	6.31	6.03	6.27	6.28	1.85*	1.70*	1.59*	1.69*	1.91*	1.43*	2.07*	0.26*	1.99*		

All values are given in valence-units (*vu*); bond-valence parameters taken from Gagné, Hawthorne (2015); *the site occupancies were considered.

Table 6 *Comparison of Voronoi-Dirichlet polyhedra volumes for Pb^{2+}-, Ca^{2+}- and Ba^{2+}-populated polyhedra for wölsendorfite.*

Mineral	Reference	Site	V_{VDP} [Å^3]	*Occ. of Ba^{2+}/ Ca^{2+}*
wölsendorfite	this paper	Pb1	16.19	0
		Pb2	17.75	0
		Pb3	17.55	0
		Pb4	17.41	0
		Pb5	16.85	0
		Pb6	17.64	0
		Ca7/Pb7	15.92	0.68
		Pb8	17.98	0
wölsendorfite	Burns (1999)	Pb1	17.76	0
		Pb2	17.35	0
		Pb3	16.97	0
		Pb4	16.97	0
		Pb5	17.06	0
		Pb6	18.61	0
		Pb7	*	
		Ba8/Pb8	22.77	0.36

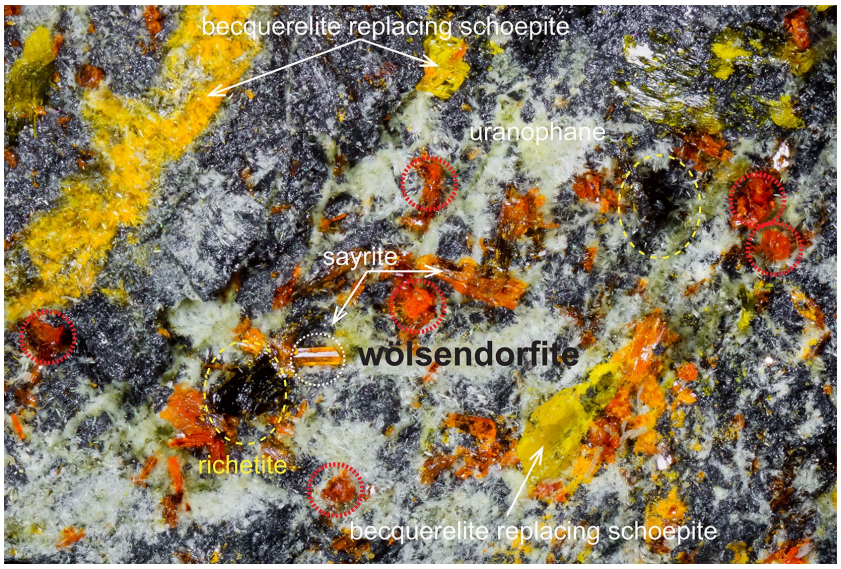

Fig. 3 *Mineral association (type I) involving studied wölsendorfite crystal (marked by red dashed circle at the center of the photography) on the holotype specimen of sayrite (RGM 13944) deposited in the collections of the Royal Museum for Central Africa in Tervuren (Belgium). The matrix of the specimen consists of more or less massive pitchblende. The horizontal field of view is 2 mm. Photo by Eddy Van Der Meersche.*

Fig. 4 *Mineral association (type II) involving wölsendorfite (reddish-orange) associated with a radial aggregate of sharpite. The Shinkolobwe mine, Haut-Katanga province, the Democratic Republic of Congo, specimen no. RMG2768, Royal Museum for Central Africa, Tervuren, Belgium. The horizontal field of view is 28 mm. Photo by Eddy Van Der Meersche.*

Some remarks on the mineral association of wölsendorfite

Wölsendorfite belongs to not so abundantly occurring uranyl minerals, although it has been reported from more than thirty localities worldwide. Most usually, it occurs as a part of the massive aggregates of UOH minerals, usually forming mixtures with other U^{6+}-containing supergene minerals, such as uranyl phosphates (metatorbernite, metaautunite) and uranyl silicates (uranophane-α, weeksite, soddyite). These aggregates were called *gummites* in the past, and this descriptive name has been retained. Wölsendorfite that forms crystals is much rarer and has been reported only from few localities. These include Shinkolobwe mine in Haut-Katanga province, Democratic Republic of Congo (Deliens et al. 1981). The vast of well-crystallized specimens originate from there. Based on the visual observations made on the reliably characterized specimens from the museum collections (MHN Luxembourg and RMCA Tervuren), some remarks can be made on the mineral association that involves wölsendorfite and related minerals and have, hopefully, a wider validity.

As has been noticed, wölsendorfite occurs as a relative late supergene phase in the alteration sequence after pitchblende. The occasional contents of Ba^{2+} and Ca^{2+} (see Burns 1999; Sejkora et al. 1997) suggest the role of alteration solutions derived from the weathered host rocks. Those elements are usually not available in the very early stages of uraninite alteration. The late stage of alteration, at least from Shinkolobwe, is usually represented by the presence of wölsendorfite, sayrite and richetite, and time-to-time also becquerelite and less also curite (usually as the massive aggregates). The other uranyl minerals comprise extremely rare

Table 7 *Most complex uranyl-oxide hydroxy-hydrate minerals and their characteristic complexity measures including H atoms.*

Mineral	Chemical formula	References	Space group	V [Å^3]	v	I_G [bits/atom]	$I_{G,total}$ [bits/cell]
vandendriesscheite	$Pb_{1.5}[(UO_2)_{10}O_6(OH)_{11}](H_2O)_{11}$	Burns (1997)	*Pbca*	8490	672	6.39	4295.64
gauthierite	$KPb[(UO_2)_7O_5(OH)_7](H_2O)_8$	Olds et al. (2017)	$P2_1/c$	5772	520	7.02	3651.63
wölsendorfite	$\mathbf{Pb_{6.07}Ca_{0.68}[(UO_2)_{14}O_{18}(OH)_5]O_{0.5}(H_2O)_{12.6}}$	**this paper**	***Cmcm***	10890	346	5.78	2000.38
richetite	$(Fe^{2+}_{0.31}Mg_{0.19})Pb_{4.86}[U^{5+}(U^{6+}O_2)_{17}O_{18}(OH)_{14}](H_2O)_{\sim 19.5}$	Plášil (2017)	*P*–1	3601	279	7.13	1988.63
schoepite	$[(UO_2)_4O(OH)_6](H_2O)_6$	Plášil (2018)	*Pbca*	3528	344	5.43	1866.64

sharpite, $Ca[(UO_2)_3(CO_3)_{3.6}O_{0.2}](H_2O)_3$, and urancalcarite, $Ca(UO_2)_3(CO_3)(OH)_6(H_2O)_3$. Rutherfordine, $UO_2(CO_3)$, is ubiquitous and does not necessarily occur with one particular mineral association.

Two specific associations warrant further comments. The first association comprises wölsendorfite, richetite, sayrite, masyuite, becquerelite, uranophane-α and, surprisingly, also schoepite. All those above-mentioned grow on a massive pitchblende. This association is extremely typical and can be easily recognized. One more extensive set of specimens (including that used in the current study) is preserved in RMCA in Tervuren and has been donated to the museum by Roger Van Dooren (La Hulpe, Belgium). It goes about the same mineral collector who donated the holotype specimen of sayrite (RGM 13944). On the fractures of massive uraninite or its veinlets, the most abundant supergene minerals are uranophane-α and becquerelite. There are also some relics of schoepite. Nevertheless, it seems that it is somewhat corroded, i.e., the rest of, at least UOHs, are younger than schoepite. The remaining association includes sayrite and richetite (Fig. 3). Wölsendorfite appears as isolated crystals or their twins. The color is very similar to that of sayrite. In fragments, it was nearly impossible to discern among them without X-ray diffraction. The second association (Fig. 4), which is also Ca-rich, is represented by rare mineral sharpite, forming radial aggregates consisting of long-prismatic needle-like crystals, rounded by thick tabular wölsendorfite. The Ba-rich association, at least from Shinkolobwe, comprises distinct minerals, including billietite. Wölsendorfite often forms crusts and partially also isolated crystals, which are, nevertheless, overgrown by uranophane-α.

Additionally, the three particularly interesting occurrences of wölsendorfite, have to be mentioned: Slavkovice nearby Nové Město na Moravě, Czechia (Sejkora et al. 1997), uranium deposits Zálesí nearby Javorník and Jelení vrch nearby Bílá Voda (Mrázek, Novák 1984). Sejkora et al. (1997) gave results of qualitative chemical analyses for wölsendorfite, which had been found along with billietite. Interestingly, they do not report the contents of Ba in wölsendorfite, but Ca instead. It can be explained that billietite formed independently, before wölsendorfite, which usually forms minute crystals in the cavities of the strongly weathered veinlets of UOHs and pitchblende. For wölsendorfite from Zálesí and Jelení vrch, only qualitative chemistry has been given. To conclude, the new modern analytical research, including both micro- and trace-elements determination, would be exciting and would help reveal the limits of the metal-cation substitutions in wölsendorfite in general.

Acknowledgments

I would like to express my thanks for providing me with great microphotographs to Eddy Van Der Meersche (Ghent, Belgium). Simon Philippo (MHN Luxembourg, Luxembourg) and Florias Mees (RMCA Tervuren, Belgium) are highly acknowledged for making samples for the research available. An anonymous referee and Jiří Čejka are acknowledged for their comments. This work was financially supported by the Ministry of Education, Youth and Sports National sustainability program I of the Czech Republic (project No. LO1603).

References

Burns PC (1999) A new complex sheet of uranyl polyhedra in the structure of wölsendorfite. Am Mineral 84: 1661–1673

Burns PC (2005) U^{6+} minerals and inorganic compounds: Insights into an expanded structural hierarchy of crystal structures. Can Mineral 43(6): 1839–1894

Burns PC, Finch RJ (1999) Wyartite: Crystallographic evidence for the first pentavalent-uranium mineral. Am Mineral 84: 1456–1460

Burns PC, Finch RJ, Hawthorne FC, Miller ML, Ewing RC (1997) The crystal structure of ianthinite, $[U_2^{4+}(UO_2)_4O_6(OH)_4(H_2O)_4](H_2O)_5$: a possible phase for Pu^{4+} incorporation during the oxidation of spent nuclear fuel. J Nucl Mater 249: 199–206

Deliens M, Piret P, Comblain G (1981) Les minéraux secondaires d'uranium du Zaïre. Published by Musée Royal de l'Afrique Central, Tervuren, Belgium.

Ewing RC (2015) Long-term storage of spent nuclear fuel. Nature Mater 14: 252–257

Finch RJ, Ewing RC (1992) The corrosion of uraninite under oxidizing conditions. J Nucl Mater 190: 133–156

Finch RJ, Murakami T (1999) Systematics and paragenesis of uranium minerals. In: Burns PC, Finch RJ (eds) Uranium: Mineralogy, Geochemistry and the Environment. Rev Mineral Geochem 38: 91–180

Finch RJ, Burns PC, Hawthorne FC, Ewing RC (2006) Refinement of the crystal structure of billietite $Ba[(UO_2)_6O_4(OH)_6](H_2O)_8$. Can Mineral 44: 1197–1205

Gurzhiy VV, Plášil J (2019) Structural complexity of natural uranyl sulfates. Acta Crystallogr B 75: 39–48

Gurzhiy VV, Kuporev IV, Kovrugin VM, Murashko MN, Kasatkin AV, Plasil J (2019) Crystal chemistry and structural complexity of natural and synthetic uranyl selenites. Crystals 9: 639

Klingensmith AL, Deely KM, Kinman WS, Kelly V, Burns PC (2007) Neptunium incorporation in sodium-substituted metaschoepite. Am Mineral 92: 662–669

Krivovichev SV (2012) Topological complexity of crystal structures: quantitative approach. Acta Crystallogr A 68: 393–398

Krivovichev SV (2013) Structural complexity of minerals: information storage and processing in the mineral world. Mineral Mag 77: 275–326

Krivovichev SV (2014) Which inorganic structures are the most complex? Angew Chem Int Ed Engl 53: 654–661

Krivovichev SV (2016) Structural complexity and configurational entropy of crystals. Acta Crystallogr B 72: 274–276

Krivovichev SV (2020) Polyoxometalate clusters in minerals: review and complexity analysis. Acta Crystallogr B 76, 618–629

Krivovichev SV, Plášil J (2013) Mineralogy and crystallography of uranium. In: Burns P. C., Sigmon G. E. (eds) Uranium: From Cradle to Grave. Mineralogical Association of Canada Short Courses 43, pp 15–119

Kubatko KA, Helean K, Navrotsky A, Burns PC (2006) Thermodynamics of uranyl minerals: Enthalpies of formation of uranyl oxide hydrates. Am Mineral 91: 658–666

Lussier AJ, Lopez RAK, Burns PC (2016) A revised and expanded structure hierarchy of natural and synthetic hexavalent uranium compounds. Can Mineral 54: 177–283

Maher K, Bargar JR, Brown GE Jr (2013) Environmental speciation of actinides. Inorg Chem 52: 3510–3532

Mrázek Z, Novák M (1984) Secondary minerals of uranium from Zálesí and Horní Hoštice in the Rychlebské hory Mts., northern Moravia. Acta Mus Moraviae, Sci Nat 69: 7–35 (in Czech)

Murakami T, Ohnuki T, Isobe H, Sato T (1997) Mobility of uranium during weathering. Am Mineral 88: 888–899

O'Hare PAG, Lewis BM, Nguyen SN (1988) Thermochemistry of uranium compounds XVII. Standard molar enthalpy of formation at 198.15 K of dehydrated schoepite UO3·0.9H2O. Thermodynamics of (schoepite + dehydrated schoepite + water). J Chem Thermodyn 20: 1287–1296

Olds TA, Plášil J, Kampf AR, Škoda R, Burns PC, Čejka J, Bourgoin V, Boulliard J-C (2017a) Gauthierite, $KPb[(UO_2)_7O_5(OH)_7]\cdot 8H_2O$, a new uranyl-oxide hydroxy-hydrate mineral from Shinkolobwe with a novel uranyl-anion sheet topology. Eur J Mineral 29: 129–141

Olds TA, Plášil J, Kampf AR, Simonetti A, Sadergaski LR, Chen YS, Burns PC (2017b) Ewingite: Earth's most complex mineral. Geology 45: 1007–1010

Pagoaga MK, Appleman DE, Stewart JM (1987) Crystal structures and crystal chemistry of the uranyl oxide hydrates becquerelite, billietite, and protasite. Am Mineral 72: 1230–1238

Petříček V, Dušek M, Palatinus L (2014) Crystallographic computing system JANA2006: General features. Z Kristallogr 229: 345–352

Plášil J (2014) Oxidation–hydration weathering of uraninite: the current state-of-knowledge. J Geosci 59: 99–114

Plášil J (2017) Crystal structure of richetite revisited: Crystallographic evidence for the presence of pentavalent uranium. Am Mineral 102: 1171–1175

Plášil J (2018a) Uranyl-oxide hydroxy-hydrate minerals: their structural complexity and evolution trends. Eur J Mineral 30: 237–251

Plášil J (2018b) The crystal structure of uranyl-oxide mineral schoepite, $[(UO_2)_4O(OH)_6]$ $(H_2O)_6$, revisited. J Geosci 63: 65–73

Plášil J, Sejkora J, Ondruš P, Veselovský F, Beran P, Goliáš V (2006) Supergene minerals in the Horní Slavkov uranium ore district, Czech Republic. J Czech Geol Soc 51: 149–158

Plášil J, Sejkora J, Čejka J, Škoda R, Goliáš V (2009) Supergene mineralization of the Medvědín uranium deposit, Krkonoše Mountains, Czech Republic. J Geosci 54: 15–56

Plášil J, Kampf AR, Škoda R, Čejka J (2018) Nollmotzite, $Mg[U^{V}(U^{VI}O_2)_2O_4F_3]\cdot 4H_2O$, the first natural uranium oxide containing fluorine. Acta Crystallogr B 74: 362–369

Plášil J, Kampf AR, Olds TA, Sejkora J, Škoda R, Burns PC, Čejka J (2020) The new K, Pb-bearing uranyl -oxide mineral kroupaite: Crystal-chemical implications for the structures of uranyl-oxide hydroxy-hydrates. Am Mineral 105: 561–568

Protas J (1957) La wölsendorfite, nouvelle espèce uranifère. C R Hebd Séan Acad Sci 244: 2942–2944

Rigaku (2019) CrysAlis CCD and CrysAlis RED. Oxford Diffraction Ltd, Yarnton, Oxfordshire, UK

Sejkora J, Mazuch J, Abert F, Šrein V, Novotná M (1997) Supergene mineralization of the Slavkovice uranium deposit in western Moravia. Acta Mus Moraviae, Sci Nat 81: 3–24 (in Czech)

Sheldrick GM (2015) Crystal structure refinement with SHELXL. Acta Crystallogr C 71: 3–8